Atomic-Scale Investigation of Graphene Grown on Cu Foil and the Effects of Thermal Annealing

Jongweon Cho,[†,*] Li Gao,[†] Jifa Tian,[‡,§] Helin Cao,[‡,§] Wei Wu,[⊥] Qingkai Yu,[⊥,¶] Esmeralda N. Yitamben,[†] Brandon Fisher,[†] Jeffrey R. Guest,[†] Yong P. Chen,[‡,§] and Nathan P. Guisinger[†]

[†]Center for Nanoscale Materials, Argonne National Laboratory, Argonne, Illinois 60439, United States , [‡]Department of Physics, Purdue University, West Lafayette, Indiana 47907, United States , [§]Birck Nanotechnology Center, Purdue University, West Lafayette, Indiana 47907, United States , and [⊥]Center for Advanced Materials and Department of Electrical and Computer Engineering, University of Houston, Houston, Texas 77204, United States . [¶] Present address: Ingram School of Engineering and Materials Science, Engineering and Commercialization Program, Texas State University, San Marcos, Texas 78666, United States.

ABSTRACT We have investigated the effects of thermal annealing on *ex-situ* chemically vapor deposited submonolayer graphene islands on polycrystalline Cu foil at the atomic-scale using ultrahigh vacuum scanning tunneling microscopy. Low-temperature annealed graphene islands on Cu foil (at ~430 °C) exhibit predominantly striped Moiré patterns, indicating a relatively weak interaction between graphene and the underlying polycrystalline Cu foil. Rapid high-temperature annealing of the sample (at 700−800 °C) gives rise to the removal of Cu oxide and the recovery of crystallographic features of the copper that surrounds the intact graphene. These experimental observations of continuous crystalline features between the underlying copper (beneath the graphene islands) and the surrounding exposed copper areas revealed by high-temperature annealing demonstrates the impenetrable nature of graphene and its potential application as a protective layer against corrosion.

KEYWORDS: graphene · chemical vapor deposition · Cu foil · scanning tunneling microscopy · Moiré pattern · corrosion · surface oxide

Graphene, a single atomic layer of covalently bonded carbon atoms, is a remarkable two-dimensional electron system that exhibits novel physical properties[1,2] and has recently been the focus of numerous research efforts.[3−5] While a number of different methods for graphene synthesis are being explored including the micromechanical cleavage of graphite,[6] epitaxial growth on SiC,[7] the dispersion of graphite in organic solvents,[8] and thermal decomposition of hydrocarbons on transition metal surfaces,[9] recent reports of graphene synthesis on Cu foil *via* chemical vapor deposition (CVD) are promising due to large-scale synthesis at low cost, self-limiting monolayer formation, and relatively facile capability of transfer to other substrates.[10,11] To improve the quality of graphene films on Cu foil prepared by CVD and better understand its microscopic growth, atomic-scale characterization becomes of great importance for both fundamental science and technological applications. To date, atomic-scale investigations on this system are rather few.[12−14]

Thermal annealing has been widely employed as one of the experimental control knobs for a number of condensed matter systems, and graphene is no exception. It has been extensively used for graphene on various substrates in order to remove any possible contamination and thus improve sample cleanliness (for example, exfoliated graphene on SiO_2 at below 400 °C in Ar atmosphere[15] or in ultrahigh vacuum (UHV)[16]). However, systematic study of the thermal annealing effect on CVD-grown graphene on Cu foil has not been addressed.

We have used a UHV scanning tunneling microscopy (STM) to characterize the structural properties of CVD-grown graphene on Cu foil at the nanoscale and atomic-scale caused by heat-treatment. We find that prolonged low-temperature annealing of the sample (at ~430 °C) reveals predominantly striped Moiré patterns, suggesting relatively weak interaction between graphene and Cu foil. Because the growth of the graphene is done *ex situ*, any exposed regions of Cu foil, where graphene has not grown, becomes oxidized. These regions have an amorphous appearance, while atomic steps and crystalline feature of the Cu foil are preserved in the regions with a graphene overlayer. It is very clear that the graphene is protecting the underlying substrate from oxidation. High-temperature annealing of the sample (at 700−800 °C) results in full recovery of the crystallinity and morphology of the exposed Cu foil area that surrounds the graphene islands and was previously amorphous in nature. This simple demonstration and observation clearly shows that the robust, impenetrable,

* Address correspondence to jwcho@anl.gov.

Received for review December 6, 2010 and accepted April 18, 2011.

Published online April 18, 2011
10.1021/nn103338g

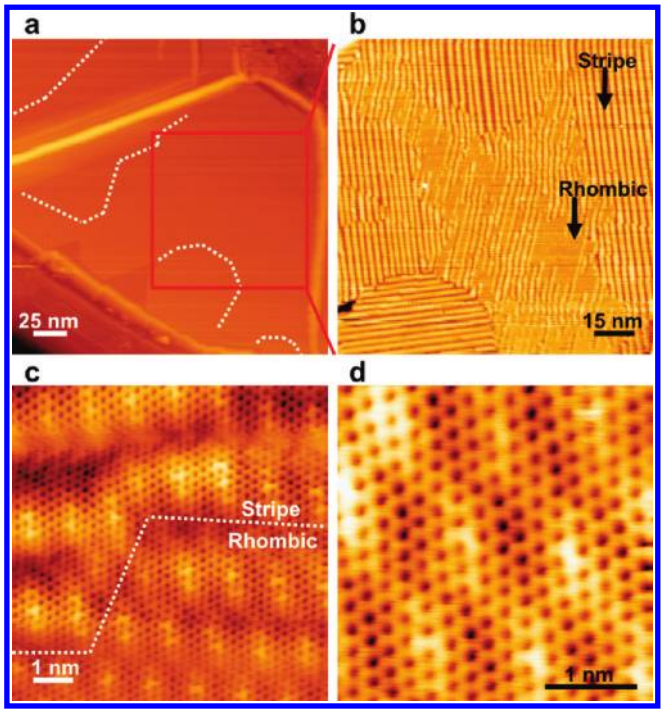

Figure 1. STM topographic images of graphene islands on Cu foil after prolonged low-temperature annealing: (a) a large field of view of a representative graphene island with some domain boundaries highlighted by white dashed lines (100 pA, −1 V), (b) a close-up view of the red box indicated in panel a (100 pA, −1 V), (c) a close-up view of a different graphene island at a pattern boundary (indicated by white dashed line) where the stripe pattern (top) and the rhombic pattern (bottom) converge (100 pA, −1 V), (d) high-resolution STM image of panel c showing honeycomb graphene lattice (3 nA, −0.5 V).

and inert nature of graphene makes it an excellent protective layer aagainst corrosion.

RESULTS AND DISCUSSION

Prior to a systematic study of thermal annealing, we explored graphene islands grown on Cu foil after undergoing prolonged thermal cycling at ~430 °C (>100 h) in UHV. At various stages of annealing, the graphene islands were imaged, as illustrated in Figure 1a, where the upper right-hand corner shows a small region of exposed oxidized Cu. The characterization of the graphene regions revealed a predominant display of striped patterns within the graphene islands, as shown in STM topographic images (Figure 1a,b). These patterns appear to have periodicity of 2.5 ± 0.2 nm between adjacent stripes. These observed features in the graphene appear to be Moiré patterns resulting from the mismatch of the hexagonal graphene lattice with crystalline domains of the Cu foil that are cubic close-packed in nature. It is key to note that the bulk foil substrate is polycrystalline, but at these small length scales we are able to probe regions of single crystal domains within the Cu foil substrate. Moiré patterns have been experimentally seen in graphene overlayer systems[17] including graphene on single crystal Ir,[18,19] Ru,[20,21] Pt,[22] and Cu.[23,24] We also frequently observe a 90° rotation of the stripe pattern resulting in orthogonally oriented stripes whose boundaries typically run at ~120°, as some of these boundaries are highlighted in Figure 1a.

We also observe a secondary Moiré pattern that appears to have a rhombic structure, which is distinctly different from the predominant stripe pattern, as shown in Figure 1b. The rhombic pattern appears to have periodicities of 1.4 ± 0.1 nm and 1.2 ± 0.1 nm with a relative angle of 75 ± 5°. We note that the presence of the rhombic patterns in our experimental data statistically appears to be relatively local and less frequent compared to the predominant striped patterns. Figure 1c shows a close-up view of a different graphene island where the stripe pattern (top) and the rhombic pattern (bottom) converge. When we further zoom in on these pattern boundaries, the graphene honeycomb lattice is clearly visible within each pattern domains (Figure 1c,d), and does not appear to be influenced by large-scale periodic patterns.

To gain detailed insight into the atomic structure of the two observed patterns, we have performed simple simulations by superimposing two rotationally mismatched lattices, that is, the graphene and Cu surface. We first discuss our simulation results for the predominantly observed stripe patterns. Due to the polycrystalline nature of the Cu surface and the symmetry of the stripe patterns we take into account the low-index crystallographic orientations such as Cu(100) and Cu(110), and vary the relative orientation between graphene and Cu lattices for simulation. Figure 2a depicts the simulated patterns generated from graphene and Cu(100) with a relative angle of 0° (atomic

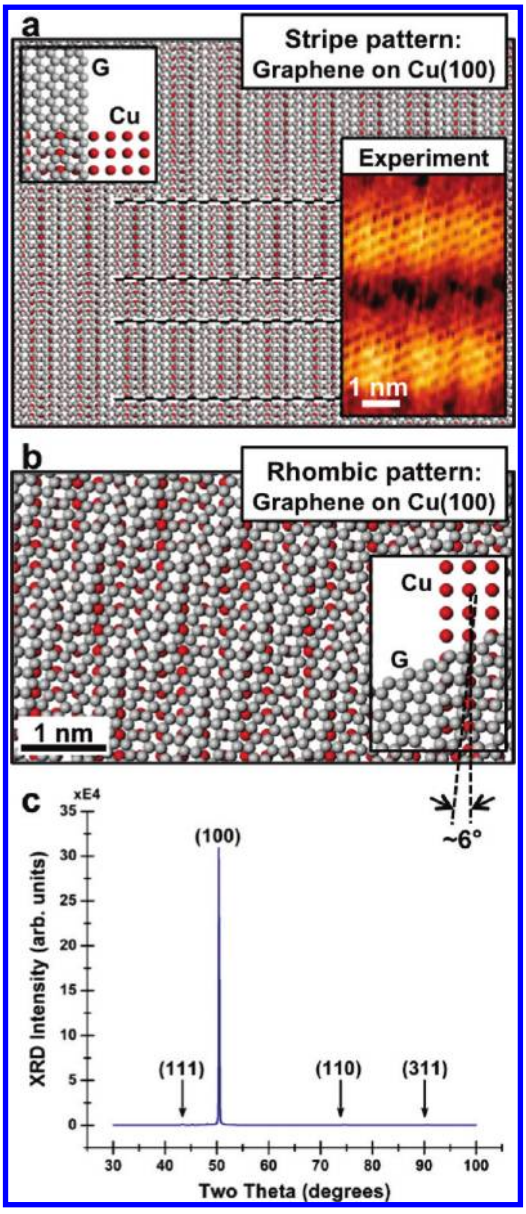

Figure 2. (a) Simulation of the predominantly observed stripe patterns with graphene and copper lattice: upper left inset shows atomic structure model with 0° relative orientation between graphene and Cu(100) and lower right inset shows the experimental STM topographic image scaled correctly with the model. Simulated patterns are in quite acceptable agreement with superimposed experimental STM image in terms of large (2.5 ± 0.2 nm) and small (1.2 ± 0.1 nm) periodic modulations of stripe patterns (dashed lines are extended from our experimental data to serve as a guide to the eye for the large-scale modulation). Image was acquired with *I* = 1 nA, V = −400 mV. (b) Simulation of the rhombic patterns with graphene and Cu(100) lattices: lower right inset shows atomic structure model with relative orientation of ∼6° with respect to that of striped patterns. Simulated patterns are in good agreement with the experimental data shown in Figure 1c,d in terms of both their periodicities and their relative orientation. In panels a and b, graphene and Cu(100) lattices are indicated by "G" and "Cu", respectively. (c) XRD spectra measured on the same sample which displayed the predominant striped Moiré pattern in Figure 1 (after further annealing at 700 °C for 10 min): the exclusively dominant peak at ∼50.5° corresponds to (100) crystallographic orientation of the Cu foil.

structure shown in the upper left inset), which are in quite acceptable agreement with superimposed experimental data (note there is also a periodic modulation of 1.2 ± 0.1 nm along each stripe). We find that Cu(110) does not reproduce both large and small scale modulations present in the observed striped patterns. Moreover, X-ray diffraction (XRD) measurements that we performed on the same sample indicate the dominant signal associated with Cu(100) crystallographic domains, as shown in Figure 2c. These simulations in tandem with the XRD measurements further support our claim that the stripe patterns are indicative of Moiré patterns, resulting from the superposition of the graphene and the Cu lattices. The deviation of our experimentally observed periodicities of stripe patterns from the exact overlay of two lattices is likely due to the strain (*e.g.*, see the pronounced changes in periodicity of the stripe patterns in the upper part of Figure 1b). We now discuss our simulation results for the locally and less frequently observed rhombic patterns. We find that Moiré patterns arising from the Cu(100) domain overlaid with graphene lattice with rotational disorder (∼6°) with respect to atomic arrangements of the striped patterns result in good agreement with the experimental data (see Figure 2b and Figure 1c,d). Our model is consistent with (i) the relatively small difference in the measured corrugation amplitude (root-mean-square roughness of ∼30 pm) on each area of the two Moiré patterns and (ii) the continuous appearance of graphene lattice across the boundary of the two patterns without indication of the presence of stepped facet surface areas, as can be seen in the STM image of Figure 1c. The fact that we have observed multiple Moiré patterns and orientations suggest that the interaction between graphene and Cu foil is relatively weak, compared to graphene on Ru(0001), where exclusively single perfect Moiré superstructures were seen.[20] Our results are consistent with graphene grown on single crystal samples[23,24] as well as the relatively low graphene−Cu(111) binding energy (33 meV per carbon atom) reported in recent theoretical investigations.[25,26] The variation of Moiré patterns observed in our graphene islands (in submonolayer regime which better captures initial stages of graphene growth on Cu foil) is also consistent with a recent STM study of full-monolayer CVD graphene grown on Cu foil.[14]

Crystallinity of the graphene films grown on Cu foil will play a crucial role in its transport properties and can affect carrier mobilities. For instance, the graphene island in Figure 1a is not single-crystalline but composed of multiple merged graphene domains. As previously discussed, evidence of multiple graphene domains comes from the observation of 120° angles of the boundaries between orthogonally oriented Moiré patterns (dashed lines in Figure 1a), implying hexagonal symmetry of the graphene lattice since the

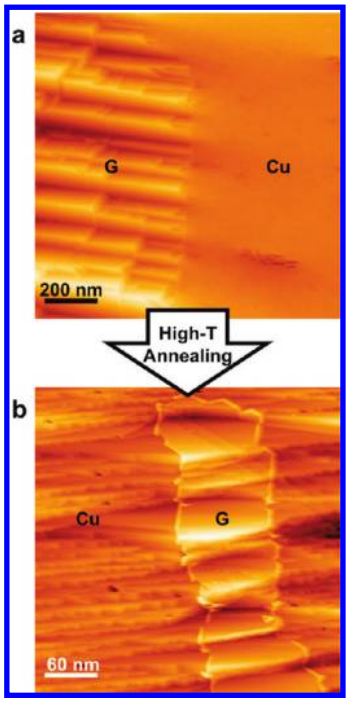

Figure 3. STM topographic images of graphene islands on Cu foil (a) before and (b) after subjected to high-temperature annealing at 700 °C for 10 min. The sample previously exhibited Moiré patterns after prolonged low-temperature annealing. Graphene island and the surrounding copper area are indicated by "G" and "Cu", respectively. Images were acquired with $I = 100$ pA at (a) $V = -1$ V and (b) $V = 2$ V, respectively.

Cu(100) surface would not have such symmetry. It is noteworthy that in the case of graphene on the Cu(100) crystallographic direction the relative orientation of 0° and 90° is identical due to its symmetry, and thus any apparent orthogonality of adjacent striped Moiré patterns does not necessarily imply existence of a domain boundary of different underlying Cu crystallographic orientations. Furthermore, as we conduct prolonged thermal annealing of our sample at ~430 °C in UHV, we expect the foil becomes more crystalline,[27] thereby leading to much larger Cu crystalline domains than the observed domain size of Moiré patterns. These graphene films with multiple domains are consistent with the domains that are observed in graphene on single crystal Cu(111),[23] and thus different graphene platelets from different nucleation sites are expected to merge during graphene growth. We also believe that the graphene shown in Figure 1c, however, is single-crystalline since we do not observe enhanced electron scattering taking place at the boundary,[23] but there is a change in the Moiré pattern (stripe *vs* rhombic structure), resulting from (i) local strain on graphene overlayer or (ii) local disorder on the domains in the underlying Cu substrate.

When the sample is subjected to thermal annealing at higher temperatures (≥700 °C) by electron bombardment in UHV, we find that the morphology of exposed Cu foil area that surrounds the graphene islands drastically changes while preserving the graphene. Figure 3a depicts an STM topographic image of a graphene island on Cu foil before high-temperature annealing. The sample was previously exposed to air for sample transfer and other *ex-situ* characterizations, and underwent a series of low-temperature annealing (≤430 °C). The graphene island indicated, G, appears to have preserved the highly faceted atomic structure of the underlying Cu foil. The surrounding exposed copper area, Cu, which appears to be oxidized, is amorphous with a distinct discontinuity at the graphene island boundary. Figure 3b shows an STM topographic image of the same sample (not the same spot) acquired after it was subjected to electron-beam heating at 700 °C for 10 min. Now the Cu foil (Cu) that surrounds the graphene islands (G) exhibits atomic steps and terraces while preserving the graphene overlayer. We believe that a thin oxide, as well as some residual hydrocarbons, was removed by high-temperature annealing, which was likely formed when the sample was exposed to atmosphere for sample transfer and other characterizations performed outside the UHV chamber. However, we cannot exclude the possibility of partial formation of an oxide layer on the Cu foil during the graphene growth in the CVD furnace, due to the growth in a nonoptimum environment.

As shown in Figure 3a,b, the morphology and crystallographic features of the underlying Cu foil beneath the graphene island, which was preserved by graphene formation, is now continuously connected to the surrounding Cu foil area following high temperature annealing. This observed connectivity experimentally demonstrates that the graphene overlayer is a superior protective coating particularly for materials that easily oxidize in an uncontrolled way when exposed to air. This is the first direct demonstration of excellent oxidation-resistant properties of graphene through the nanometer-scale imaging, showing the protective property of graphene persists up to the boundaries of submonolayer graphene films.[28] We note in passing that there is a significant demand for protective thin-film coatings which can prevent oxidation processes becoming increasingly important in a number of technological applications.

To investigate the evolution of the surface morphology as a function of the annealing temperature, we performed a systematic study of a thermal annealing experiment in UHV. We started with a freshly prepared sample of graphene grown on Cu foil in the CVD furnace, transferred it into the UHV chamber, and heated the sample step-by-step at specific temperatures while keeping the annealing time the same (14 h for 400−600 °C range and 20 min for 700−800 °C range). Here we note that the exposure of the sample to air is unavoidable due to *ex-situ* sample preparation, which would cause surface oxidization of Cu foil. Figure 4 shows a series of representative STM topographic

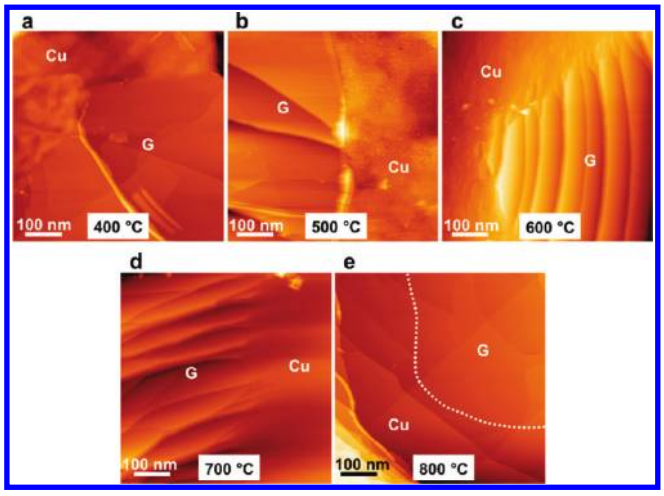

Figure 4. Sequential STM topographic images of the same sample subjected to successive thermal annealing at specified temperatures ranging from 400 to 800 °C. Graphene and Cu areas are indicated by "G" and "Cu", respectively. In panel e, the boundary between the graphene island and Cu foil is indicated by a white dashed line, where the assignment of the graphene island is made on the basis of the spatially resolved d*I*/d*V* map simultaneously taken with the topographic image (see text along with Figure 5). Images were acquired with (a) *I* = 50 pA, *V* = −1 V, (b) *I* = 50 pA, *V* = −1 V, (c) *I* = 50 pA, *V* = −2 V, (d) *I* = 100 pA, *V* = −2 V, and (e) *I* = 100 pA, *V* = −700 mV, respectively.

images (with the same image size) of the same sample after the annealing temperature is sequentially increased. The morphological evolution of the Cu area displays the occurrence of crossover from its amorphous appearance (Figure 4a, annealed at 400 °C) to the appearance of the Cu atomic steps (Figure 4e, annealed at 800 °C), whereas graphene islands still preserve the underlying Cu atomic steps and atomically smooth basal terraces that were previously formed during the graphene growth (note the high-temperature environment of graphene growth at ~1050 °C). While we observe the continuously connected crystalline features after thermal annealing at 700 °C (see Supporting Information Figure S1), we find that the annealing temperature should be further increased (up to 800 °C) to see the continuity in the relatively large flat areas (with terraces of a few hundred nanometers). The annealing at 800 °C results in the complete removal of oxide formed on exposed Cu regions and the continuity of crystalline features is now clearly seen for large sample areas, when Figure 4d and Figure 4e are compared. The surface morphology changes observed during this evolution unambiguously demonstrate the ability of graphene, a single atom-thick carbon layer, to prohibit surface oxidation from taking place and provides the evidence that the high-temperature heat-treatment significantly improves overall sample cleanliness. The surface is comparable to studies done on expensive single crystals.

After the sample is subjected to thermal annealing at elevated temperatures around 700−800 °C, thereby leading to the observation of atomic steps of the surrounding Cu surface area, it is no longer straightforward to identify graphene islands from the copper surface, based on solely large-scale STM topographic images (without further efforts to zoom in on sampled

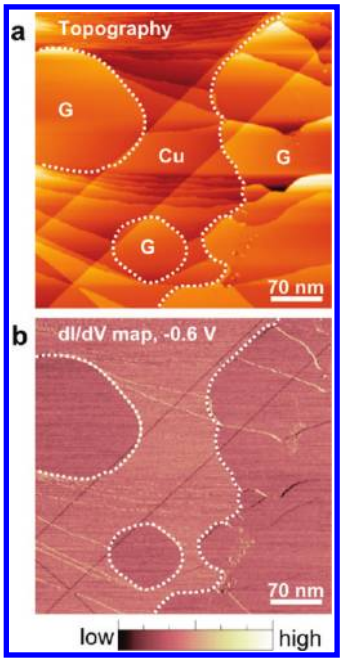

Figure 5. STM topography and differential conductance d*I*/d*V* image of graphene on Cu foil annealed at 800 °C: (a) STM topographic image showing graphene area (indicated by "G") and Cu area (indicated by "Cu"), (b) simultaneously acquired d*I*/d*V* map using a lock-in amplifier. Both images were acquired with *I* = 100 pA, *V* = −600 mV.

areas and acquire atomic-resolution images). For correct identification of the surface areas with heterogeneous materials, we conducted simultaneous measurement of differential conductance d*I*/d*V* map with topography, which represent a spatial mapping of the local density of states (LDOS) of the surface.[29] Figure 5 shows both STM topographic image and d*I*/d*V* map (taken at −600 meV) taken at the same area of the sample after thermal annealing at 800 °C for 20 min

(the same sample used in Figure 4). Figure 5b reveals substantial electronic contrast differences arising from graphene and Cu foil, which allows us to directly correlate them to the surface morphologies. This assignment is further confirmed by the atomic-scale image of hexagonal lattice in the graphene area.

CONCLUSIONS

We have used a UHV STM to investigate effects of thermal annealing on CVD-grown graphene on Cu foil at the atomic scale. We observe predominantly stripe Moiré patterns after prolonged low-temperature annealing. Continuous crystalline features between copper beneath graphene islands and the surrounding copper area are elucidated through high-temperature annealing. Our systematic study of the evolution of the surface morphology while the annealing temperature is varied suggests that graphene overlayer offers the potential for a protective layer against the oxidation of metals.

EXPERIMENTAL METHODS

STM characterization was performed using a home-built variable temperature STM in a UHV chamber at a base pressure of $<2 \times 10^{-10}$ mbar. STM measurements were made by using electrochemically etched W tips and at a substrate temperature of 45 K. Differential conductance d*I*/d*V* images were acquired through a lock-in technique with an ac modulation signal of 20−30 mV (rms) at 10 kHz simultaneously with STM topographic images. STM images were processed using WSxM[30] without smoothing or FFT filtering. Graphene islands were grown by CVD (CH_4 as carbon stock) on Cu foils at ambient pressure following the procedure described in ref 13: (1) cleaning a Cu foil (25-μm-thick, 99.8%, Alfa Aesar) at 1050 °C for 30 min under 300 sccm Ar and 10 sccm H_2 in a CVD furnace, and (2) subsequently growing graphene at 1050 °C for ∼10 min (short enough so the graphene islands have not merged to form a continuous film) under 300 sccm CH_4 (8 ppm in Ar) and 10 sccm of H_2. Both resistive and electron-beam heating were employed to investigate effects of thermal annealing on the sample in UHV. Sample temperature was monitored using either thermocouples or an infrared pyrometer depending on the heating method. XRD data were collected using a Bruker D8 Discover diffractometer with a Cu X-ray source, concentric Eulerian cradle, Göbel detector, and scintillation detector.

Acknowledgment. The use of the Center for Nanoscale Materials at Argonne National Laboratory was supported by the U.S. Department of Energy, Office of Science, Office of Basic Energy Sciences, under Contract No. DE-AC02-06CH11357 and "SISGR" Contract No. DE-FG02-09ER16109. This work is also supported by DARPA contract MIPR 10-E533.

Supporting Information Available: One figure of STM image of the highly stepped sample area after thermal annealing at 700 °C. This material is available free of charge *via* the Internet at http://pubs.acs.org.

REFERENCES AND NOTES

1. Novoselov, K. S.; Geim, A. K.; Morozov, S. V.; Jiang, D.; Zhang, Y.; Dubonos, S. V.; Grigorieva, I. V.; Firsov, A. A. Electric Field Effect in Atomically Thin Carbon Films. *Science* **2004**, *306*, 666–669.
2. Zhang, Y. B.; Tan, Y. W.; Stormer, H. L.; Kim, P. Experimental Observation of the Quantum Hall Effect and Berry's Phase in Graphene. *Nature* **2005**, *438*, 201–204.
3. Geim, A. K.; Novoselov, K. S. The Rise of Graphene. *Nat. Mater.* **2007**, *6*, 183–191.
4. Castro Neto, A. H.; Guinea, F.; Peres, N. M. R.; Novoselov, K. S.; Geim, A. K. The Electronic Properties of Graphene. *Rev. Mod. Phys.* **2009**, *81*, 109–162.
5. Geim, A. K. Graphene: Status and Prospects. *Science* **2009**, *324*, 1530–1534.
6. Novoselov, K. S.; Jiang, D.; Schedin, F.; Booth, T. J.; Khotkevich, V. V.; Morozov, S. V.; Geim, A. K. Two-Dimensional Atomic Crystals. *Proc. Natl. Acad. Sci. U.S.A.* **2005**, *102*, 10451–10453.
7. Berger, C.; Song, Z. M.; Li, T. B.; Li, X. B.; Ogbazghi, A. Y.; Feng, R.; Dai, Z. T.; Marchenkov, A. N.; Conrad, E. H.; First, P. N.; *et al.* Ultrathin Epitaxial Graphite: 2D Electron Gas Properties and a Route toward Graphene-Based Nanoelectronics. *J. Phys. Chem. B* **2004**, *108*, 19912–19916.
8. Hernandez, Y.; Nicolosi, V.; Lotya, M.; Blighe, F. M.; Sun, Z. Y.; De, S.; McGovern, I. T.; Holland, B.; Byrne, M.; Gun'ko, Y. K.; *et al.* High-Yield Production of Graphene by Liquid-Phase Exfoliation of Graphite. *Nat. Nanotechnol.* **2008**, *3*, 563–568.
9. Kim, K. S.; Zhao, Y.; Jang, H.; Lee, S. Y.; Kim, J. M.; Kim, K. S.; Ahn, J. H.; Kim, P.; Choi, J. Y.; Hong, B. H. Large-Scale Pattern Growth of Graphene Films for Stretchable Transparent Electrodes. *Nature* **2009**, *457*, 706–710.
10. Li, X. S.; Cai, W. W.; An, J. H.; Kim, S.; Nah, J.; Yang, D. X.; Piner, R.; Velamakanni, A.; Jung, I.; Tutuc, E.; *et al.* Large-Area Synthesis of High-Quality and Uniform Graphene Films on Copper Foils. *Science* **2009**, *324*, 1312–1314.
11. Bae, S.; Kim, H.; Lee, Y.; Xu, X. F.; Park, J. S.; Zheng, Y.; Balakrishnan, J.; Lei, T.; Kim, H. R.; Song, Y. I.; *et al.* Roll-to-Roll Production of 30-Inch Graphene Films for Transparent Electrodes. *Nat. Nanotechnol.* **2010**, *5*, 574–578.
12. Yeh, N.-C.; Teague, M. L.; Yeom, S.; Standley, B. L.; Boyd, D. A.; Bockrath, M. W. Strain-Induced Pseudomagnetic Fields and Charging Effects on CVD-Grown Graphene. 2010, arXiv:1009.0081. arXiv.org e-Print archive. http://arxiv.org/abs/1009.0081 (accessed November 24, 2010).
13. Yu, Q. K.; Jauregui, L. A.; Wu, W.; Colby, R.; Tian, J.; Su, Z.; Cao, H.; Liu, Z.; Pandey, D.; Wei, D.; *et al.* Control and Characterization of Individual Grains and Grain Boundaries in Graphene Grown by Chemical Vapor Deposition. *Nat. Mater.* **2011**, in press.
14. Rasool, H. I.; Song, E. B.; Allen, M. J.; Wassei, J. K.; Kaner, R. B.; Wang, K. L.; Weiller, B. H.; Gimzewski, J. K. Continuity of Graphene on Polycrystalline Copper. *Nano Lett.* **2011**, *11*, 251–256.
15. Elias, D. C.; Nair, R. R.; Mohiuddin, T. M. G.; Morozov, S. V.; Blake, P.; Halsall, M. P.; Ferrari, A. C.; Boukhvalov, D. W.; Katsnelson, M. I.; Geim, A. K.; *et al.* Control of Graphene's Properties by Reversible Hydrogenation: Evidence for Graphane. *Science* **2009**, *323*, 610–613.
16. Zhang, Y. B.; Brar, V. W.; Wang, F.; Girit, C.; Yayon, Y.; Panlasigui, M.; Zettl, A.; Crommie, M. F. Giant Phonon-Induced Conductance in Scanning Tunnelling Spectroscopy of Gate-Tunable Graphene. *Nat. Phys.* **2008**, *4*, 627–630.
17. Wintterlin, J.; Bocquet, M. L. Graphene on Metal Surfaces. *Surf. Sci.* **2009**, *603*, 1841–1852.
18. Coraux, J.; N'Diaye, A. T.; Busse, C.; Michely, T. Structural Coherency of Graphene on Ir(111). *Nano Lett.* **2008**, *8*, 565–570.
19. Balog, R.; Jorgensen, B.; Nilsson, L.; Andersen, M.; Rienks, E.; Bianchi, M.; Fanetti, M.; Laegsgaard, E.; Baraldi, A.; Lizzit, S.; *et al.* Bandgap Opening in Graphene Induced by Patterned Hydrogen Adsorption. *Nat. Mater.* **2010**, *9*, 315–319.
20. Marchini, S.; Gunther, S.; Wintterlin, J. Scanning Tunneling Microscopy of Graphene on Ru(0001). *Phys. Rev. B* **2007**, *76*, 075429.
21. N'Diaye, A. T.; Bleikamp, S.; Feibelman, P. J.; Michely, T. Two-Dimensional Ir Cluster Lattice on a Graphene Moire on Ir(111). *Phys. Rev. Lett.* **2006**, *97*, 215501.

22. Land, T. A.; Michely, T.; Behm, R. J.; Hemminger, J. C.; Comsa, G. STM Investigation of Single Layer Graphite Structures Produced on Pt(111) by Hydrocarbon Decomposition. *Surf. Sci.* **1992**, *264*, 261–270.
23. Gao, L.; Guest, J. R.; Guisinger, N. P. Epitaxial Graphene on Cu(111). *Nano Lett.* **2010**, *10*, 3512–3516.
24. Zhao, L.; Rim, K. T.; Zhou, H.; He, R.; Heinz, T. F.; Pinczuk, A.; Flynn, G. W.; Pasupathy, A. N. The Atomic-Scale Growth of Large-Area Monolayer Graphene on Single-Crystal Copper Substrates. arXiv:1008.3542.
25. Giovannetti, G.; Khomyakov, P. A.; Brocks, G.; Karpan, V. M.; van den Brink, J.; Kelly, P. J. Doping Graphene with Metal Contacts. *Phys. Rev. Lett.* **2008**, *101*, 026803.
26. Khomyakov, P. A.; Giovannetti, G.; Rusu, P. C.; Brocks, G.; van den Brink, J.; Kelly, P. J. First-Principles Study of the Interaction and Charge Transfer Between Graphene and Metals. *Phys. Rev. B.* **2009**, *79*, 195425.
27. Holm, E. A.; Foiles, S. M. How Grain Growth Stops: A Mechanism for Grain-Growth Stagnation in Pure Materials. *Science* **2010**, *328*, 1138–1141.
28. After submission of this report, we became aware of a recent experimental work showing corrosion-resistant aspect of graphene using scanning electron microscopy, X-ray photoelectron spectroscopy, and Raman spectroscopy at the micron scale: Chen, S.; Brown, L.; Levendorf, M.; Cai, W.; Ju, S.; Edgeworth, J.; Li, X.; Magnuson, C. W.; Velamakanni, A.; Piner, R. D.; *et al*. Oxidation Resistance of Graphene-Coated Cu and Cu/Ni Alloy. *ACS Nano* **2011**, *5*, 1321–1327.
29. Tersoff, J.; Hamann, D. R. Theory of the Scanning Tunneling Microscope. *Phys. Rev. B* **1985**, *31*, 805–813.
30. Horcas, I.; Fernandez, R.; Gomez-Rodriguez, J. M.; Colchero, J.; Gomez-Herrero, J.; Baro, A. M. WSXM: A Software for Scanning Probe Microscopy and a Tool for Nanotechnology. *Rev. Sci. Instrum.* **2007**, *78*, 013705.